Integrating Robust CRT with Signal Unwrapping for Modulo Sampling

Chutong Shen, Wenyi Yan, *Graduate Student Member, IEEE*, Yimin D. Zhang, *Fellow, IEEE*, and Lu Gan, *Senior Member, IEEE*

***Abstract*—Two-channel modulo sampling based on the robust Chinese remainder theorem (RCRT) enables closed-form, point-wise reconstruction, yet its recovery remains fundamentally limited by the effective RCRT threshold. This letter addresses this limitation through a hybrid architecture that integrates RCRT-based recovery with difference-based unwrapping. The RCRT stage is reinterpreted as a coarse modulo operator with an expanded threshold, while the difference stage resolves the residual ambiguity by exploiting temporal structure. The proposed scheme extends recovery beyond the intrinsic RCRT range and simultaneously relaxes the oversampling requirement for a fixed difference order. Theoretical analysis establishes the resulting sampling condition, and the effectiveness of the proposed method is validated through both simulations and hardware experiments.**

***Index Terms*—Modulo sampling, modulo analog-to-digital converter (ADC), high dynamic range, signal reconstruction.**

I. Introduction

Modulo sampling, also known as unlimited sampling, exploiting modulo analog-to-digital converters (ADCs) has recently attracted great interest as an efficient approach for high-dynamic-range signal acquisition [1]–[14]. By folding large-amplitude signals into a bounded interval $[-\lambda, \lambda)$ at the hardware level, modulo sampling avoids clipping, while subsequent reconstruction algorithms recover the original signal [15]–[22].

In the single-channel setting, several reconstruction strategies have been developed. The original unlimited sampling framework leverages high-order finite differences (HoD) to suppress wrapping prior to signal unwrapping [2], yielding a simple pipeline with linear-time complexity. More recent methods improve robustness by exploiting additional structure through Fourier Prony method [23], iterative refinement [24], or sparse residual recovery. While these approaches tolerate challenging noise conditions and operate at lower oversampling rates for moderate dynamic ranges (e.g., amplitude scaling factors ≤ 10), they incur increased computational cost. Moreover, all methods still require high oversampling factors when the signal amplitude is large.

A complementary approach employs multi-channel sampling [25]–[29] based on the robust Chinese remainder theorem (RCRT) [30]–[33]. By combining two modular measurements, RCRT enables stable and closed-form point-wise reconstruction. However, this capability remains fundamentally bounded: Once the signal exceeds the effective RCRT threshold, it cannot be unambiguously reconstructed. In addition, increasing the dynamic range requires precise hardware matching of large coprime moduli, which is challenging due to analog nonidealities and calibration limits [34]–[36].

To overcome the hard range limit of RCRT while avoiding the high-order instability of standalone HoD-based unwrapping, we propose a hybrid reconstruction framework, termed *RCRT–HoD*.

The key insight is to reinterpret the RCRT output as a coarse modulo signal with an expanded *virtual threshold*, where the RCRT stage acts as a *virtual modulo ADC* that reduces the amplitude scale factor before passing the residual to the HoD backend. Our main contributions are summarized as follows:

- A formal proof that RCRT fusion preserves the modular structure at an expanded threshold, introducing the concept of a virtual effective threshold and enabling the reinterpretation of RCRT as a modulo front-end.
- Derivation of sampling conditions for the hybrid architecture under both noiseless and noisy settings, showing that the effective amplitude scaling factor is significantly reduced, thereby relaxing the oversampling requirement.
- Simulation and hardware experimental results validating that RCRT–HoD extends the dynamic range beyond the conventional RCRT ceiling with low computational cost.

II. System Model and Preliminaries

A. Signal Model

Let $g(t) \in PW_\Omega$ denote a signal in the Paley-Wiener space, consisting of real-valued continuous-time functions bandlimited to $[-\Omega, \Omega]$ rad/s. The signal is sampled uniformly with sampling interval $T > 0$. The resulting discrete-time sample sequence is denoted by $\gamma[k] \triangleq g(kT)$ for $k \in \mathbb{Z}$. Throughout this letter, we assume that the sampling interval satisfies the Nyquist criterion $T \leq \pi/\Omega$, ensuring that $g(t)$ is uniquely determined by its samples.

Let $\|g\|_\infty \triangleq \sup_{t\in\mathbb{R}} |g(t)|$ denote the signal amplitude bound. The analog front-end is assumed to have a finite voltage range characterized by a threshold $\lambda > 0$, where the high-dynamic-range regime of interest corresponds to $\|g\|_\infty \gg \lambda$.

To facilitate the analysis of sampling-rate requirements, we define the dimensionless amplitude scaling factor ρ and the oversampling factor OF as:

$$\rho \triangleq \frac{\|g\|_\infty}{\lambda} \quad \text{and} \quad \mathrm{OF} \triangleq \frac{f_s}{f_{\mathrm{Nyq}}}, \tag{1}$$

where $f_s = 1/T$ is the sampling rate and $f_{\mathrm{Nyq}} = \Omega/\pi$ denotes the Nyquist rate of $g(t)$.

C. Shen and Y. D. Zhang are with the Department of Electrical and Computer Engineering, Temple University, Philadelphia, PA 19122, USA.

W. Yan and L. Gan are with the Department of Engineering, Brunel University of London, UK.

B. Modulo Sampling and HoD Baseline

Unlike conventional saturation, a modulo-based acquisition front-end folds the signal amplitude into a bounded range. The centered modulo operator $\mathcal{M}_\lambda : \mathbb{R} \to [-\lambda, \lambda)$ is defined as [2]

$$\mathcal{M}_\lambda(x) \triangleq 2\lambda\left(\left[\left[\frac{x}{2\lambda}+\frac{1}{2}\right]\right]-\frac{1}{2}\right), \tag{2}$$

where $[[u]] \triangleq u - \lfloor u \rfloor$ denotes the fractional part of u with $\lfloor\cdot\rfloor$ being the floor function. Applying $\mathcal{M}_\lambda(\cdot)$ to $g(t)$ yields the discrete-time modulo samples:

$$y[k] \triangleq \mathcal{M}_\lambda(\gamma[k]), \quad k \in \mathbb{Z}. \tag{3}$$

HoD-based unwrapping recovers $\{\gamma[k]\}$ from $\{y[k]\}$ by exploiting the smoothness of bandlimited signals [2]. Let Δ^N denote the N-th order forward finite-difference operator, defined as:

$$\Delta^N\gamma[k] \triangleq \sum_{i=0}^{N}(-1)^{N-i}\binom{N}{i}\gamma[k+i]. \tag{4}$$

This operator approximates the scaled N-th order derivative of a discrete-time signal. Recent work [37] has derived a tightened bound on the finite differences of bandlimited signals, improving upon classical results by removing the factor of e:

$$\|\Delta^N\gamma\|_\infty \le (T\Omega)^N\|g\|_\infty. \tag{5}$$

When the difference order N is chosen such that $\|\Delta^N\gamma\|_\infty < \lambda$, the effects of modulo folding are eliminated in the difference domain, enabling unique reconstruction of $\gamma[k]$.

This sufficient condition highlights the fundamental trade-off between T, N, and ρ, and serves as the single-channel baseline against which the proposed two-channel architecture is evaluated.

C. Two-Channel Modulo Sampling via RCRT

We consider a two-channel modulo sampling architecture based on RCRT, which utilizes structured redundancy to expand the unambiguous dynamic range. Two centered modulo operators with distinct thresholds $\lambda_1 = \Gamma_1 M$ and $\lambda_2 = \Gamma_2 M$ are applied to the same signal $g(t)$, where Γ_1 and Γ_2 are coprime integers with $\lambda_2 > \lambda_1$ (i.e., $\Gamma_2 > \Gamma_1$), and M is a common real-valued scaling factor. The resulting samples are $y_\ell[k] = \mathcal{M}_{\lambda_\ell}(\gamma[k])$ for $\ell \in \{1, 2\}$.

The pair $\{y_1[k], y_2[k]\}$ admits a unique reconstruction of $\gamma[k] = g(kT)$ provided that the amplitude remains within a significantly larger effective threshold, defined as:

$$\lambda_{\text{eff}} \triangleq \operatorname{lcm}(\Gamma_1, \Gamma_2)M = \Gamma_1\Gamma_2 M, \tag{6}$$

where $\operatorname{lcm}(\cdot,\cdot)$ denotes the least common multiple operation. Specifically, RCRT guarantees exact recovery if $|g(kT)| < \lambda_{\text{eff}}$. However, standard RCRT fails to reconstruct signals exceeding this limit (i.e., $|g(kT)| \ge \lambda_{\text{eff}}$), effectively imposing a hard ceiling on the measurable dynamic range.

III. Proposed Hybrid Architecture: Extending RCRT with Difference-Based Unwrapping

While the RCRT provides a closed-form solution for multi-channel modulo sampling, its recovery capability is fundamentally bounded by λ_{eff}, beyond which catastrophic wrapping errors occur. To overcome this ceiling, we propose a hybrid architecture that cascades the RCRT front-end with HoD-based backend unwrapping. By reinterpreting the RCRT output as a coarse modulo signal, the effective amplitude bound is significantly expanded, while inheriting the relaxed sampling constraints of the RCRT stage.

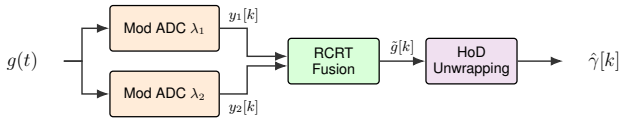

Fig. 1: System block diagram of the proposed hybrid RCRT-HoD architecture.

A. RCRT as a Modulo Front-End

Fig. 1 shows the block diagram of the proposed pipeline which cascades RCRT fusion with HoD-based unwrapping. The RCRT output serves as the input to the subsequent HoD-based unwrapping stage, which then restores an estimate of $\gamma[k]$, denoted as $\hat{\gamma}[k]$, by resolving the remaining ambiguity in the difference domain.

We establish the following proposition to rigorously describe the behavior of the fused output when the signal exceeds the individual channel ranges.

Proposition 1 (Consistency of Modulo Reconstruction)**.** *Let the channel thresholds be $\lambda_l = \Gamma_l M$ for $l \in \{1, 2\}$, where Γ_1 and Γ_2 are coprime integers with $\Gamma_2 > \Gamma_1$, and $M \in \mathbb{R}^+$ is a common real-valued scaling factor. Let $\lambda_{\text{eff}} = \Gamma_1\Gamma_2 M$. For any two real-valued numbers x and $\hat{x}$, if $\mathcal{M}_{\lambda_l}(x) = \mathcal{M}_{\lambda_l}(\hat{x})$ holds for both $l \in \{1, 2\}$, then $\mathcal{M}_{\lambda_{\text{eff}}}(x) = \mathcal{M}_{\lambda_{\text{eff}}}(\hat{x})$.*

Proof. From $\mathcal{M}_{\lambda_l}(x) = \mathcal{M}_{\lambda_l}(\hat{x})$ for $l \in \{1, 2\}$, there exist integers n_1 and n_2 such that

$$x - \hat{x} = 2\lambda_1 n_1 = 2\lambda_2 n_2 \implies \Gamma_1 n_1 = \Gamma_2 n_2, \tag{7}$$

where the implication follows by substituting $\lambda_l = \Gamma_l M$ and dividing by $2M$. Since the greatest common divisor of Γ_1 and Γ_2 is $\gcd(\Gamma_1, \Gamma_2) = 1$, n_1 can be divided by Γ_2, i.e., $n_1 = k\Gamma_2$ for some $k \in \mathbb{Z}$. Therefore,

$$x - \hat{x} = 2\Gamma_1 M(k\Gamma_2) = 2k\lambda_{\text{eff}}, \tag{8}$$

and $\mathcal{M}_{\lambda_{\text{eff}}}(x) = \mathcal{M}_{\lambda_{\text{eff}}}(\hat{x})$ follows immediately. □

Remark. *When $M = 1/2$, the thresholds reduce to $\lambda_l = \Gamma_l/2$ for $l \in \{1, 2\}$, and the modulo operation $\mathcal{M}_{\lambda_l}(\cdot)$ corresponds to the standard remainder modulo Γ_l for integer-valued inputs. The proposition thus extends this classical result to real-valued inputs and two real-scaled moduli.*

Proposition 1 shows that the RCRT stage effectively functions as a single virtual modulo ADC with a larger threshold λ_{eff} to handle signals exceeding the point-wise RCRT recovery range. The resulting effective-modulo signal is expressed as

$$\tilde{g}[k] \triangleq \mathcal{M}_{\lambda_{\text{eff}}}\big(\gamma[k]\big) \in [-\lambda_{\text{eff}}, \lambda_{\text{eff}}), \tag{9}$$

which serves as the input to the subsequent HoD-based unwrapping stage.

Fig. 2 illustrates a bandlimited signal where the RCRT output $\tilde{g}[k]$ behaves as a centered modulo mapping. In this example, an effective threshold of $\lambda_{\text{eff}} = 15.5$ V is obtained for a bandlimited signal with $\Omega = 10\pi$ rad/s from two channels with much lower thresholds of $\lambda_1 = 0.5$ V and $\lambda_2 = 0.62$ V.

B. Relaxed Sampling Conditions with Fixed Order

We now quantify the sampling efficiency improvement. We fix the difference order N, as large N amplifies noise exponentially by 2^N [37], thereby limiting its practical range.

For a conventional single-channel HoD-based unwrapping system with threshold λ_2, the sufficient condition for noiseless recovery is determined by the signal's amplitude scaling factor $\rho_{\text{base}} = \|g\|_\infty/\lambda_2$. Leveraging the tightened bound from [37], the required baseline oversampling factor is:

$$\text{OF}_{\text{base}} > \pi(\rho_{\text{base}})^{1/N}. \tag{10}$$

In the proposed hybrid architecture, the RCRT front-end expands the threshold to $\lambda_{\text{eff}} \gg \lambda_2$, significantly reducing the effective amplitude scaling factor. Substituting $\lambda_2 = \Gamma_2 M$ and $\lambda_{\text{eff}} = \Gamma_1\Gamma_2 M$ yields $\lambda_{\text{eff}}/\lambda_2 = \Gamma_1$, so:

$$\rho_{\text{eff}} \triangleq \frac{\|g\|_\infty}{\lambda_{\text{eff}}} = \frac{\rho_{\text{base}}\lambda_2}{\lambda_{\text{eff}}} = \frac{\rho_{\text{base}}}{\Gamma_1}. \tag{11}$$

Since the system uses two parallel ADCs, the aggregate oversampling factor is twice the per-channel requirement. Applying (10) yields:

$$\text{OF}_{\text{hyb}} > 2\pi(\rho_{\text{eff}})^{1/N} = 2\pi\left(\frac{\rho_{\text{base}}}{\Gamma_1}\right)^{1/N}. \tag{12}$$

This reduction in ρ_{eff} distinguishes our approach from single-channel methods (e.g., signal sieving [24] or ISTA solvers [38]), which rely on costly iterative solvers for large ρ_{base}. Our architecture instead uses a simple, linear-complexity HoD operator.

C. Stability Analysis under Noise

In practice, modulo samples are subject to quantization, hysteresis delay [4], truncation, and thermal noise [7]. In this subsection, we analyze the stability of the proposed architecture under bounded post-folding measurement error. The practical sources of such errors and the scope of this model are discussed in the next subsection.

Proposition 2. *Consider the post-folding error model:*

$$\tilde{y}_l[k] = \mathcal{M}_{\lambda_l}(\gamma[k]) + e_l[k], \quad l \in \{1, 2\}, \tag{13}$$

where $e_l[k]$ denotes the post-folding measurement error. Let $\|e\|_\infty \triangleq \max_{l\in\{1,2\}} \|e_l\|_\infty$ be the maximum error amplitude across channels. Under the assumptions that $\|e\|_\infty$ is strictly bounded by the RCRT tolerance $M/2$, and the difference order N satisfies $2^N < 2\Gamma_1\Gamma_2$, the proposed architecture guarantees stable reconstruction provided that the aggregate oversampling factor satisfies:

$$\text{OF}_{\text{hyb}} > \frac{2\pi(\rho_{\text{eff}})^{\frac{1}{N}}}{1 - 2^N\frac{\|e\|_\infty}{\lambda_{\text{eff}}}}. \tag{14}$$

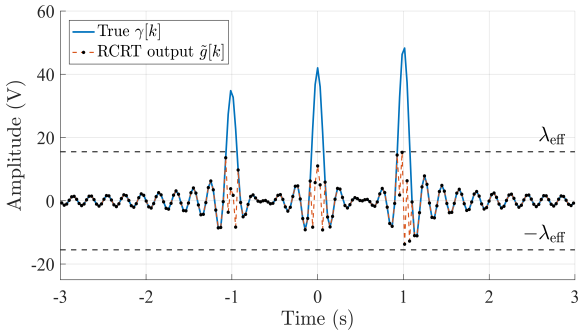

Fig. 2: RCRT output behaves as a centered modulo mapping with threshold $\lambda_{\text{eff}} = 15.5$ V from two channels with thresholds $\lambda_1 = 0.5$ V and $\lambda_2 = 0.62$ V

.

Proof. We refine the argument by distinguishing the RCRT stage and the HoD stage. First, define the effective-modulo signal $\tilde{g}[k] \triangleq \mathcal{M}_{\lambda_{\text{eff}}}(\gamma[k])$. By Proposition 1, $\gamma[k]$ and $\tilde{g}[k]$ produce identical ideal residues. Thus, the error model in (13) is equivalent to observing $\tilde{g}[k]$:

$$\tilde{y}_l[k] = \mathcal{M}_{\lambda_l}(\tilde{g}[k]) + e_l[k]. \tag{15}$$

Given the error bound $\|e\|_\infty < M/2$, the RCRT algorithm correctly recovers the folding integers of $\tilde{g}[k]$ since $\|\tilde{g}\|_\infty < \lambda_{\text{eff}}$. The fusion output $\hat{g}[k]$ therefore satisfies:

$$\hat{g}[k] = \tilde{g}[k] + \eta[k], \tag{16}$$

where $\eta[k]$ is the residual error that satisfies $\|\eta\|_\infty \leq \max_{l\in\{1,2\}} \|e_l\|_\infty = \|e\|_\infty < M/2$.

Second, we analyze the HoD-based unwrapping stage, which operates on $\hat{g}[k]$. The effective error density relative to the expanded threshold $\lambda_{\text{eff}} = \Gamma_1\Gamma_2 M$ is bounded by:

$$\rho_\eta \triangleq \frac{\|\eta\|_\infty}{\lambda_{\text{eff}}} \leq \frac{\|e\|_\infty}{\lambda_{\text{eff}}}. \tag{17}$$

Incorporating this error density into the stability bound for difference-based recovery [37] and scaling by 2 to account for the dual-channel aggregate cost, the sufficient condition becomes $\text{OF}_{\text{hyb}} > 2\pi\rho_{\text{eff}}^{1/N}/(1 - 2^N\rho_\eta)$. Substituting $\rho_\eta \leq \|e\|_\infty/\lambda_{\text{eff}}$ yields the general error-dependent bound in (14).

Notice that in the noiseless scenario ($\|e\|_\infty \to 0$), this condition seamlessly reduces to the baseline hybrid bound in (12). Furthermore, to ensure that the bound remains meaningful even under the worst-case tolerable noise ($\|e\|_\infty \to M/2$), we inherently require $2^N < 2\Gamma_1\Gamma_2$ to prevent the denominator from becoming negative, rendering the difference-domain bound meaningless. □

D. Practical Noise Sources and Limitations

Although pre-folding thermal noise is inherently unbounded and may cause spurious folds, the ADC's finite dynamic range truncates the output to $[-\lambda_l, \lambda_l)$, which bounds the post-folding error in (13). From (13), the total error satisfies

$$|e_l[k]| \leq |\tilde{y}_l[k]| + |\mathcal{M}_{\lambda_l}(\gamma[k])| \leq 2\lambda_l, \tag{18}$$

since both terms are confined to $[-\lambda_l, \lambda_l)$. For high-quality folding operators (e.g., FPGA-based), the signal-to-noise-and-distortion ratio (SINAD) can exceed 50 dB at kHz-range frequencies [37], keeping post-folding errors well within the $M/2$ tolerance. In contrast, low-cost modulo hardware [7] may exhibit significantly higher thermal noise, causing $\|e\|_\infty$ to exceed $M/2$ with high probability and leading to reconstruction failure. Both behaviours are demonstrated in the next section. Noise tolerance can be extended via additional channels, multichannel noise modelling [13], thresholding-based recovery [4], [39], [40], or maximum likelihood estimation-based RCRT [41], [42], though these are left for future work.

IV. Simulation and Hardware Results

A. Simulations

1) Noiseless case: We verify that the proposed *RCRT–HoD* architecture can reconstruct signals exceeding the effective RCRT threshold. The test signals are bandlimited to $\Omega = 10\pi$ rad/s. We set the channel thresholds to $\lambda_1 = 0.5$ V and $\lambda_2 = 0.62$ V. This corresponds to $\Gamma_1 = 25$, $\Gamma_2 = 31$, and $M = 0.02$ V, yielding an effective RCRT threshold of $\lambda_{\text{eff}} = 15.5$ V. The finite-difference order is selected at $N = 3$.

Range extension at fixed sampling rate. With $\text{OF} = 10$, we sweep the signal amplitude $\|g\|_\infty$ beyond λ_{eff}. Numerical results confirm that the RCRT-only baseline fails catastrophically once $\|g\|_\infty > 15.5$ V. In contrast, the proposed RCRT–HoD method maintains near-perfect recovery with mean squared-error of $\text{MSE} < -300$ dB throughout the entire range, empirically validating that the HoD-based unwrapping backend successfully resolves the residual ambiguities.

Oversampling rate requirement. We further quantify the sampling efficiency of the proposed architecture by searching for the minimum oversampling factor required for successful reconstruction ($\text{MSE} < -60$ dB) with fixed $N = 3$ and $\|g\|_\infty = 40$ V. The proposed RCRT–HoD method successfully achieves robust recovery at a significantly low rate of $\text{OF}_{\min} = 2.75$. A representative time-domain reconstruction at this low sampling rate is shown in Fig. 3.

2) Noisy case: A second parameter set with $\lambda_1 = 0.8$ V and $\lambda_2 = 1.0$ V ($\Gamma_1 = 4$, $\Gamma_2 = 5$, $\lambda_{\text{eff}} = 4$ V) is used for signals corrupted with Gaussian noise to provide a larger RCRT tolerance ($M/2 = 0.1$ V). Reconstruction performance is evaluated by $\text{SNR}_\text{r} = 10\log_{10}\left(\frac{\sum_k |\gamma[k]|^2}{\sum_k |\gamma[k]-\hat{\gamma}[k]|^2}\right)$ dB, where the summation is over all reconstructed samples. Table I reports the reconstruction SNR of RCRT–HoD ($N = 2$) under varying hysteresis and input SNR (SNR_in) levels. With per-channel hysteresis $h_l = 0.05\lambda_l$ ($l \in \{1, 2\}$) [4] and $\text{SNR}_\text{in} = 30$ dB, the method achieves up to 31.7 dB reconstruction SNR, while $h_l = 0.1\lambda_l$ reduces the ceiling to 25.5 dB. Under $\text{SNR}_\text{in} = 25$ dB, performance degrades to 7 dB, indicating near-failure conditions, with smaller hysteresis consistently yielding higher SNR.

B. Hardware Experiment

We validate RCRT-HoD using the hardware prototype [43] with $\lambda_1 = 0.36$ V, $\lambda_2 = 0.48$ V, $M = 0.12$, $\Gamma_1 = 3$, and $\Gamma_2 = 4$. Various signals $g(t)$ are tested by varying bandwidth B and peak $\|g(t)\|_\infty$, yielding different folding depths $\rho = \|g(t)\|_\infty/\lambda_2$ (see Table II). Since inputs exceed the RCRT range, the output is a residual modulo signal with $\lambda_{\text{eff}} = \Gamma_1\Gamma_2 M = 1.44$ V. For a fair comparison, the single-channel baselines ITER-SIS [24] and LASSO-B^{2}R^2 [38] employ a threshold of 0.48 V. Results in Table II show that RCRT-HoD achieves successful reconstruction with a moderate OF, while the baselines typically require significantly higher OF.

It is noted that this comparison is for proof-of-concept only, as RCRT-HoD uses two ADC channels while the single-channel baselines use one. The hardware experiments also employ controlled test signals; practical wideband inputs may introduce additional distortions not captured here.

TABLE I: RCRT–HoD reconstruction SNR_r in dB ($N = 2$, $\lambda_1 = 0.8$ V, $\lambda_2 = 1.0$ V, 50 trials).

h_1	h_2	OF	SNR_in	$\rho=5$		$\rho=10$		$\rho=20$	
				$b=4$	$b=6$	$b=4$	$b=6$	$b=4$	$b=6$
0.04	0.05	10	30 dB	28.5	31.5	30.5	31.7	31.4	31.7
0.04	0.05	20	25 dB	11.1	16.9	16.1	22.5	13.7	25.3
0.08	0.10	10	30 dB	24.3	25.4	25.2	25.5	25.4	25.5
0.08	0.10	20	25 dB	7.1	15.0	12.2	18.8	11.7	16.7

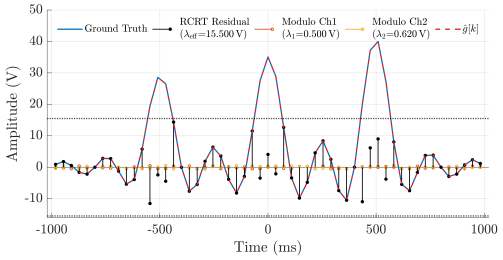

Fig. 3: Representative reconstruction of the proposed RCRT–HoD method at a low oversampling factor ($\text{OF}_{\min} = 2.75$) with $\|g\|_\infty = 40$ V.

TABLE II: Reconstruction performance (OF and SNR_r) comparison for RCRT-HoD ($\lambda_1 = 0.36$ V, $\lambda_2 = 0.48$ V), ITER-SIS, and LASSO-B^{2}R^2 across different bandwidths Ω and folding depths ρ.

Ω (krad/s)	ρ	**RCRT-HoD**		ITER-SIS [24]		LASSO-B^{2}R^2 [38]	
		OF	SNR_r	OF	SNR_r	OF	SNR_r
40π	7.2	**7.8**	29.7 dB	15.6	37.1 dB	12.5	33.7 dB
16π	10.5	**8.3**	28.6 dB	16.7	32.6 dB	31.3	26.1 dB
20π	12.8	**11.9**	24.1 dB	31.3	32.1 dB	61.3	10.1 dB

V. Conclusion

This letter proposed a hybrid framework integrating RCRT-based multi-channel fusion with HoD-based unwrapping. By exploiting the expanded effective threshold λ_{eff}, the proposed architecture significantly reduces the effective amplitude scaling factor, thereby relaxing the oversampling requirement relative to single-channel baselines. We derived theoretical stability conditions under bounded post-folding error and demonstrated that the system eliminates the dynamic range bottleneck of conventional RCRT. Simulation and hardware results confirm robust reconstruction of large-amplitude signals with a low oversampling factor.

REFERENCES

[1] A. Bhandari and F. Krahmer, "HDR imaging from quantization noise," in *Proc. IEEE Int. Conf. Image Process. (ICIP)*, Oct. 2020, pp. 101–105.

[2] A. Bhandari, F. Krahmer, and R. Raskar, "On unlimited sampling and reconstruction," *IEEE Trans. Signal Process.*, vol. 69, pp. 3827–3839, 2021.

[3] D. Florescu, F. Krahmer, and A. Bhandari, "Event-driven modulo sampling," in *Proc. IEEE Int. Conf. Acoust., Speech Signal Process. (ICASSP)*, 2021, pp. 5435–5439.

[4] ——, "The surprising benefits of hysteresis in unlimited sampling: Theory, algorithms and experiments," *IEEE Trans. Signal Process.*, vol. 70, pp. 616–630, 2022.

[5] D. Florescu and A. Bhandari, "Time encoding via unlimited sampling: Theory, algorithms and hardware validation," *IEEE Trans. Signal Process.*, vol. 70, pp. 4912–4924, 2022.

[6] R. Guo and A. Bhandari, "Unlimited sampling of FRI signals independent of sampling rate," in *Proc. IEEE Int. Conf. Acoust., Speech Signal Process. (ICASSP)*, 2023, pp. 1–5.

[7] R. Guo, Y. Zhu, and A. Bhandari, "Sub-Nyquist USF spectral estimation: k-frequencies with $6k + 4$ modulo samples," *IEEE Trans. Signal Process.*, vol. 72, pp. 5065–5076, 2024.

[8] Y. Zhu, R. Guo, P. Zhang, and A. Bhandari, "Frequency estimation via sub-Nyquist unlimited sampling," in *Proc. IEEE Int. Conf. Acoust., Speech Signal Process. (ICASSP)*, April 2024, pp. 9636–9640.

[9] V. Pavlíček, R. Guo, and A. Bhandari, "Bits, channels, frequencies and unlimited sensing: Pushing the limits of sub-Nyquist Prony," in *Proc. Eur. Signal Process. Conf. (EUSIPCO)*, 2024, pp. 2462–2466.

[10] Q. Zhang, J. Zhu, F. Qu, and D. W. Soh, "Line spectral estimation via unlimited sampling," *IEEE Trans. Aerosp. Electron. Syst.*, vol. 60, no. 5, pp. 7214–7231, 2024.

[11] D. Florescu and A. Bhandari, "Multi-dimensional unlimited sampling and robust reconstruction," *Appl. Comput. Harmon. Anal.*, vol. 79, no. 101796, pp. 1–27, 2025.

[12] R. Guo and A. Bhandari, "HoD-FP algorithm for unlimited sensing: Where time meets frequency," in *Proc. IEEE Int. Workshop Comput. Adv. Multi-Sensor Adapt. Process. (CAMSAP)*, 2025.

[13] D. Florescu, "Multichannel modulo sampling with unlimited noise," in *Proc. IEEE Int. Conf. Acoust., Speech Signal Process. (ICASSP)*, 2025, pp. 1–5.

[14] H. Wang, J. Fang, H. Li, G. Leus, R. Zhu, and L. Gan, "Line spectral estimation with unlimited sensing," *Signal Process.*, vol. 238, no. 110205, pp. 1–15, 2025.

[15] A. Bhandari, F. Krahmer, and R. Raskar, "Unlimited sampling of sparse signals," in *Proc. IEEE Int. Conf. Acoust., Speech Signal Process. (ICASSP)*, 2018, pp. 4569–4573.

[16] A. Bhandari, "Back in the US-SR: unlimited sampling and sparse super-resolution with its hardware validation," *IEEE Signal Process. Lett.*, vol. 29, pp. 1047–1051, 2022.

[17] ——, "Unlimited sampling with sparse outliers: Experiments with impulsive and jump or reset noise," in *Proc. IEEE Int. Conf. Acoust., Speech Signal Process. (ICASSP)*, 2022, pp. 5403–5407.

[18] S. Mulleti, E. Reznitskiy, S. Savariego, M. Namer, N. Glazer, and Y. C. Eldar, "A hardware prototype of wideband high-dynamic range analog-to-digital converter," *IET Circuits, Devices & Systems*, vol. 17, no. 4, pp. 181–192, 2023.

[19] G. Shtendel, D. Florescu, and A. Bhandari, "Unlimited sampling of bandpass signals: Computational demodulation via undersampling," *IEEE Trans. Signal Process.*, vol. 71, pp. 4134–4145, 2023.

[20] J. Zhu, J. Ma, Z. Liu, F. Qu, Z. Zhu, and Q. Zhang, "A modulo sampling hardware prototype and reconstruction algorithms evaluation," *IEEE Trans. Instrum. Meas.*, vol. 74, pp. 1–11, 2025.

[21] E. Romanov and O. Ordentlich, "Above the Nyquist rate, modulo folding does not hurt," *IEEE Signal Process. Lett.*, vol. 26, no. 8, pp. 1167–1171, 2019.

[22] E. Azar, S. Mulleti, and Y. C. Eldar, "Unlimited sampling beyond modulo," *Appl. Comput. Harmon. Anal.*, vol. 74, no. 101715, pp. 1–20, 2025.

[23] A. Bhandari, F. Krahmer, and T. Poskitt, "Unlimited sampling from theory to practice: Fourier-prony recovery and prototype ADC," *IEEE Trans. Signal Process.*, vol. 70, pp. 1131–1141, 2022.

[24] R. Guo and A. Bhandari, "ITER-SIS: Robust unlimited sampling via iterative signal sieving," in *Proc. IEEE Int. Conf. Acoust., Speech Signal Process. (ICASSP)*, 2023, pp. 1–5.

[25] L. Gan and H. Liu, "High dynamic range sensing using multi-channel modulo samplers," in *Proc. IEEE Sensor Array Multichannel Signal Process. Workshop (SAM)*, 2020, pp. 1–5.

[26] Y. Gong, L. Gan, and H. Liu, "Multi-channel modulo samplers constructed from Gaussian integers," *IEEE Signal Process. Lett.*, vol. 28, pp. 1828–1832, 2021.

[27] W. Yan, L. Gan, S. Hu, and H. Liu, "Towards optimized multi-channel modulo-ADCs: Moduli selection strategies and bit depth analysis," in *Proc. IEEE Int. Conf. Acoust., Speech Signal Process. (ICASSP)*, 2024, pp. 9496–9500.

[28] W. Yan, L. Gan, and Y. D. Zhang, "Threshold sensitivity in two-channel modulo ADCs: Analysis and robust reconstruction," in *Proc. IEEE Int. Conf. Acoust., Speech Signal Process. (ICASSP)*, 2025, pp. 1–5.

[29] W. Yan, Z. Li, L. Gan, H. Liu, and G. Li, "Bit-efficient quantisation for two-channel modulo-sampling systems," *IEEE Signal Process. Lett.*, pp. 1–5, 2026.

[30] X.-G. Xia and G. Wang, "Phase unwrapping and a robust Chinese remainder theorem," *IEEE Signal Process. Lett.*, vol. 14, no. 4, pp. 247–250, 2007.

[31] W. Wang and X.-G. Xia, "A closed-form robust Chinese remainder theorem and its performance analysis," *IEEE Trans. Signal Process.*, vol. 58, no. 11, pp. 5655–5666, 2010.

[32] L. Xiao, X.-G. Xia, and W. Wang, "Multi-stage robust Chinese remainder theorem," *IEEE Trans. Signal Process.*, vol. 62, pp. 4772–4785, 2014.

[33] L. Xiao, X.-G. Xia, and H. Huo, "Towards robustness in residue number systems," *IEEE Trans. Signal Process.*, vol. 65, no. 6, pp. 1497–1510, 2017.

[34] P. Harikumar and J. J. Wikner, "Design of a reference voltage buffer for a 10-bit 50 MS/s SAR ADC in 65 nm CMOS," in *Proc. IEEE Int. Symp. Circuits Syst. (ISCAS)*, 2015, pp. 249–252.

[35] B. Razavi, "The flash ADC [a circuit for all seasons]," *IEEE Solid-State Circuits Mag.*, vol. 9, no. 3, pp. 9–13, 2017.

[36] X. Tang, J. Liu, Y. Shen, S. Li, L. Shen, A. Sanyal, K. Ragab, and N. Sun, "Low-power SAR ADC design: Overview and survey of state-of-the-art techniques," *IEEE Trans. Circuits Syst. I: Regul. Pap.*, vol. 69, no. 6, pp. 2249–2262, 2022.

[37] W. Yan, Z. Li, L. Gan, H. Liu, and G. Li, "Difference-based recovery for modulo sampling: Tightened bounds and robustness guarantees," *arXiv preprint arXiv:2509.12971*, 2025.

[38] S. B. Shah, S. Mulleti, and Y. C. Eldar, "LASSO-based fast residual recovery for modulo sampling," in *Proc. IEEE Int. Conf. Acoust., Speech Signal Process. (ICASSP)*, 2023, pp. 1–5.

[39] D. Florescu and A. Bhandari, "Unlimited sampling with local averages," in *Proc. IEEE Int. Conf. Acoust., Speech Signal Process. (ICASSP)*, 2022, pp. 5742–5746.

[40] ——, "Unlimited sampling via generalized thresholding," in *Proc. IEEE Int. Symp. Inf. Theory (ISIT)*, 2022, pp. 1606–1611.

[41] X. Li, S. Sun, Q. Liao, and X.-G. Xia, "Maximum likelihood estimation-based complex-valued robust chinese remainder theorem and its fast algorithm," *IEEE J. Miniatur. Air Space Syst.*, vol. 7, no. 1, pp. 64–79, 2026.

[42] W. Wang, X. Li, W. Wang, and X.-G. Xia, "Maximum likelihood estimation based robust chinese remainder theorem for real numbers and its fast algorithm," *IEEE Trans. Signal Process.*, vol. 63, no. 13, pp. 3317–3331, 2015.

[43] Z. Li, W. Yan, R. Zhu, L. Gan, and H. Liu, "Live demonstration: real-time high-amplitude signal acquisition with 2-channel modulo ADC," in *Proc. IEEE Int. Symp. Circuits Syst. (ISCAS)*, 2025, p. 1.